

## Supporting Information

“Searching for DNA lesions: Structural evidence for lower and higher-affinity DNA binding conformations of human alkyladenine DNA glycosylase (AAG)”

Jeremy W. Setser, Gondichatnahalli M. Lingaraju, C. Ainsley Davis, Leona D. Samson,  
and Catherine L. Drennan\*

\*Correspondence should be addressed to: Catherine L. Drennan: Tel: 617-253-5622. Fax: 617-258-7847. E-mail: [cdrennan@mit.edu](mailto:cdrennan@mit.edu)

Supporting information includes: Crystallographic data collection and refinement statistics (Table S1), additional figures of the crystal structure (Figures S1 S3, and S4), and raw gel mobility shift assay data (Figure S2).

**Table S1.** Data collection and refinement statistics.

Space group	$P4_3$
Cell constants (Å)	a = b = 41.17, c = 262.55
(°)	$\alpha = \beta = \gamma = 90$
Beamline	ALS 12.3.1
Wavelength (Å)	1.116
Resolution (Å)	66 - 2.00 (2.07 - 2.00)
No. total observations	95966
No. unique observations	26998
Completeness (%) <sup>c</sup>	92.4 (89.6)
$\langle I/\sigma(I) \rangle$ <sup>c</sup>	14.8 (7.4)
$R_{\text{sym}}$ (%) <sup>a, c</sup>	7.4 (15.8)
<b>Model refinement</b>	
$R_{\text{work}}$ (%) <sup>b</sup>	21.9
$R_{\text{free}}$ (%) <sup>b</sup>	26.5
B-factors (Å <sup>2</sup> )	
Protein	35.6
DNA	48.9
Water	22.3
RMSD bonds (Å) <sup>d</sup>	0.008
RMSD angles (°) <sup>d</sup>	1.2
Number of atoms	
Protein	2965 (2 molecules/asu)
DNA	353
Water	250
Ramachandran plot (%)	
Most favored	91.0
Additionally allowed	9.0
Generously allowed	—

<sup>a</sup>:  $R_{\text{sym}} = \sum |I_{hkl} - \langle I_{hkl} \rangle| / \sum I_{hkl}$ , where  $I$  is the intensity of a reflection  $hkl$  and  $\langle I \rangle$  is the average over symmetry-related reflections of  $hkl$ .

<sup>b</sup>:  $R_{\text{work}} = \sum |F_o - F_c| / \sum |F_o|$  in which  $F_o$  and  $F_c$  are the observed and calculated structure factor amplitudes, respectively.  $R_{\text{free}}$  is calculated from 5% of the reflections not used in the model refinement.

<sup>c</sup>: Values in parenthesis correspond to the highest resolution shell.

<sup>d</sup>: RMSD, root mean square deviation.

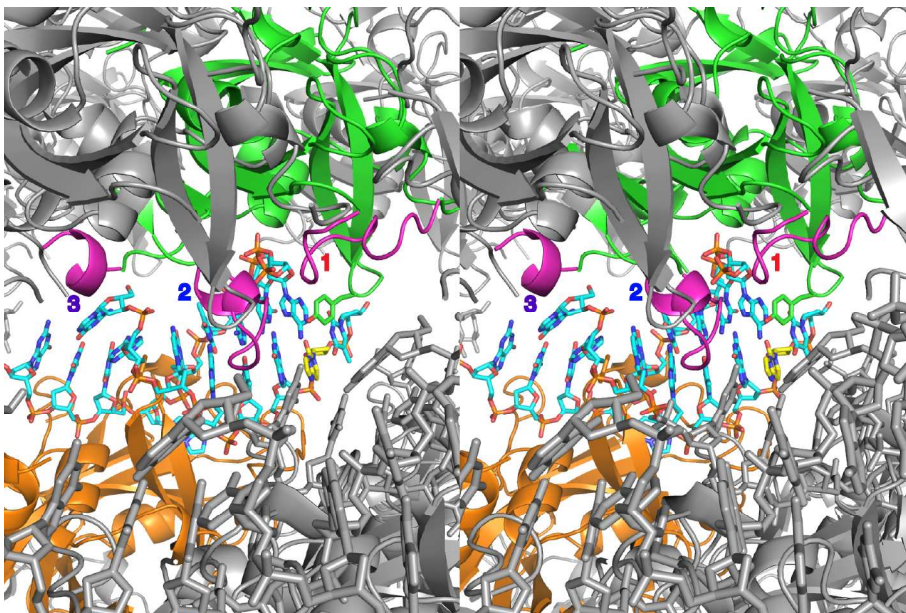


**Figure S1.** Wall-eye stereoview of the disordered loops (pink) of the lower-affinity  $\Delta 79\text{AAG}$  structure in the context of the crystal lattice. The asymmetric unit of our structure is represented as in Figure 1 with lower-affinity  $\Delta 79\text{AAG}$  and the higher-affinity pseudo-duplex structure in green and orange cartoon, respectively, with the pseudo-duplex piece of DNA between them in stick form with cyan carbons. Molecules that make up the rest of the crystal lattice are in gray with protein in cartoon and DNA in stick form. The disordered loops of lower-affinity  $\Delta 79\text{AAG}$  are visualized by aligning the  $\Delta 79\text{AAG-}\epsilon\text{A:T}$  structure (PDB ID 1F4R (1)) and displaying these loops as pink cartoon. The loops are labeled 1-3 to match the numbering scheme in Figure 3. With this view, one can see that these loops would have ample space in the crystal packing and the disorder observed in these residues is not due to crystal contacts. The  $\epsilon\text{C}$  base that is not bound in an AAG active site (in stick form with yellow carbons ( $\epsilon\text{C7}$ )) is found to have no interactions with protein (or DNA) in the crystal lattice. Non-carbon atoms are colored as follows: oxygen (red), nitrogen (blue), and phosphorus (orange).

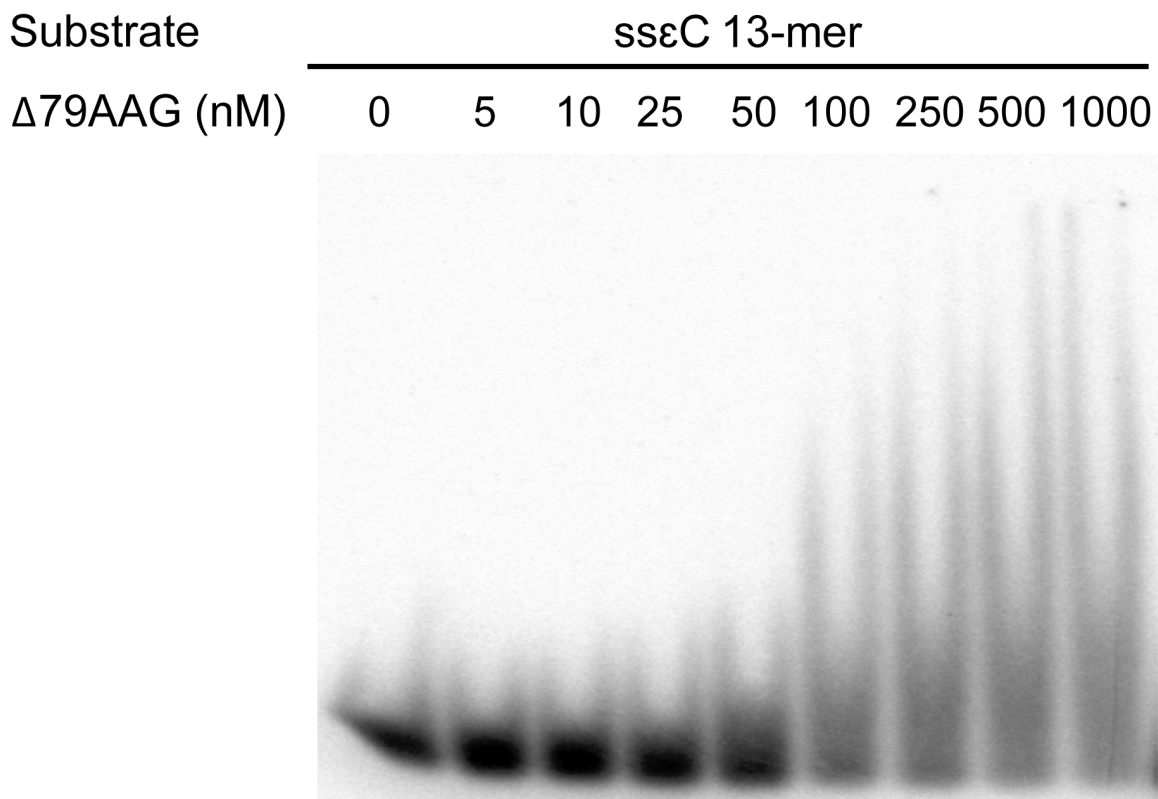


**Figure S2.** Δ79AAG shows no affinity for ssεC 13-mer by gel shift. Gel mobility shift assays were performed as previously described (2) using the indicated concentrations of Δ79AAG and 2 nM of <sup>32</sup>P-labeled ssεC 13-mer. The band at the bottom of the gel represents the ssεC 13-mer in solution. A clear band shift is not observed as the amount of Δ79AAG is increased and the smearing of the gel in the later lanes is indicative of some low-affinity interactions. This same assay performed with 13-mer duplex DNA containing the εC lesion shows a very clear band shift with a  $K_d$  of ~20 nM (2).

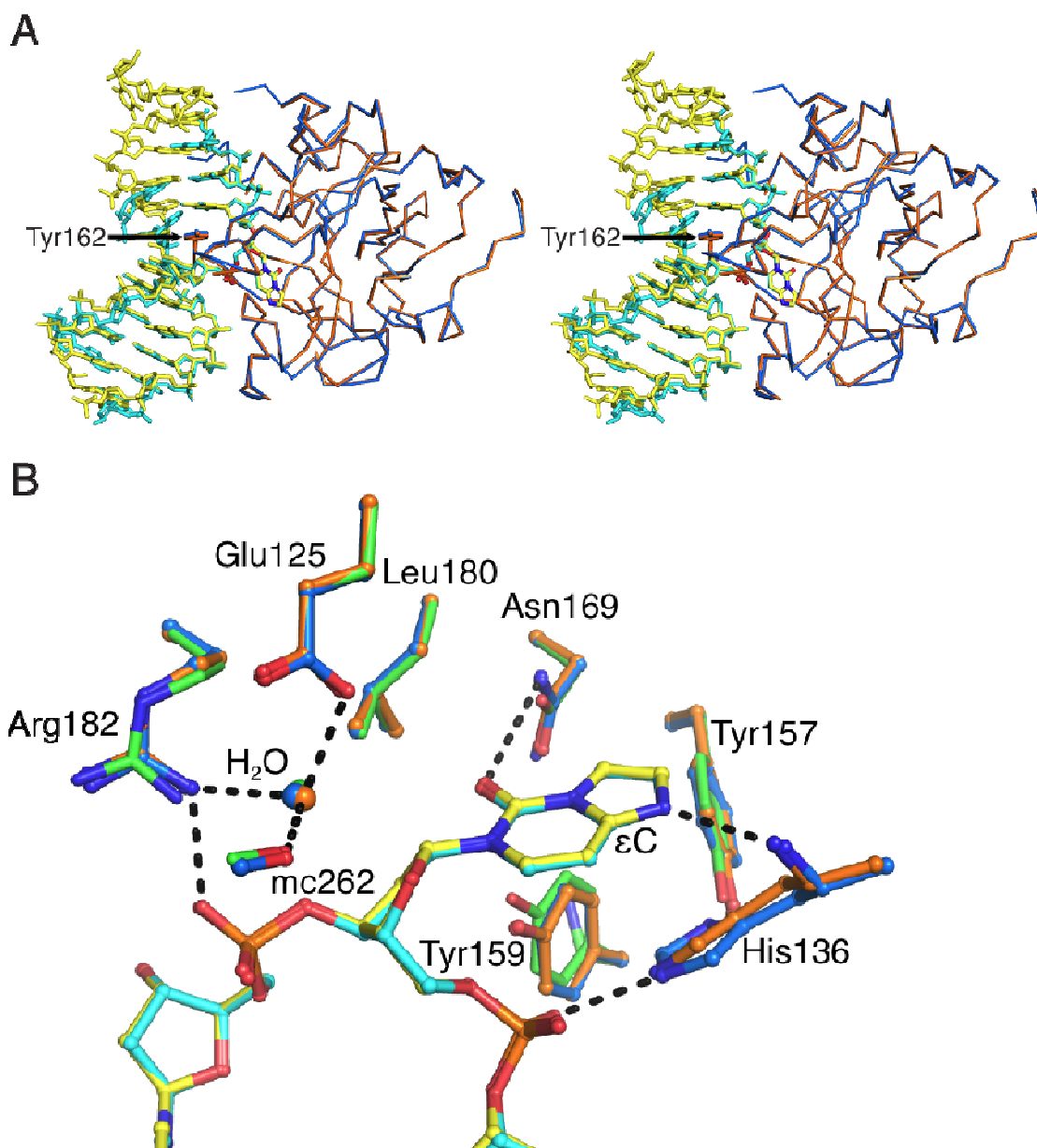


**Figure S3.**  $\Delta 79$ AAG structural comparisons. (A) A wall-eye stereoview of  $\Delta 79$ AAG bound to dsDNA (protein in blue ribbon, DNA in yellow sticks) and pseudo-duplex DNA (protein in orange ribbon, DNA in cyan sticks) shows striking similarities in binding mode. The intercalating Tyr162 (in sticks) is denoted with an arrow and the  $\epsilon$ C lesion is colored such that carbon atoms match the rest of the respective DNA. All Non-carbon atoms are colored as in Figure S1. (B) Active site overlay of  $\Delta 79$ AAG bound to  $\epsilon$ C-containing dsDNA (protein carbons in blue) and pseudo-duplex  $\epsilon$ C DNA (protein carbons in orange) with the lower-affinity structure (protein carbons in green). The putative catalytic water molecule that is present in all AAG structures is denoted as a sphere and colored to match the protein carbon atoms of its respective structure. DNA carbons and all other non-carbon atoms are colored as in (A). Hydrogen bonding is indicated as dashed lines.

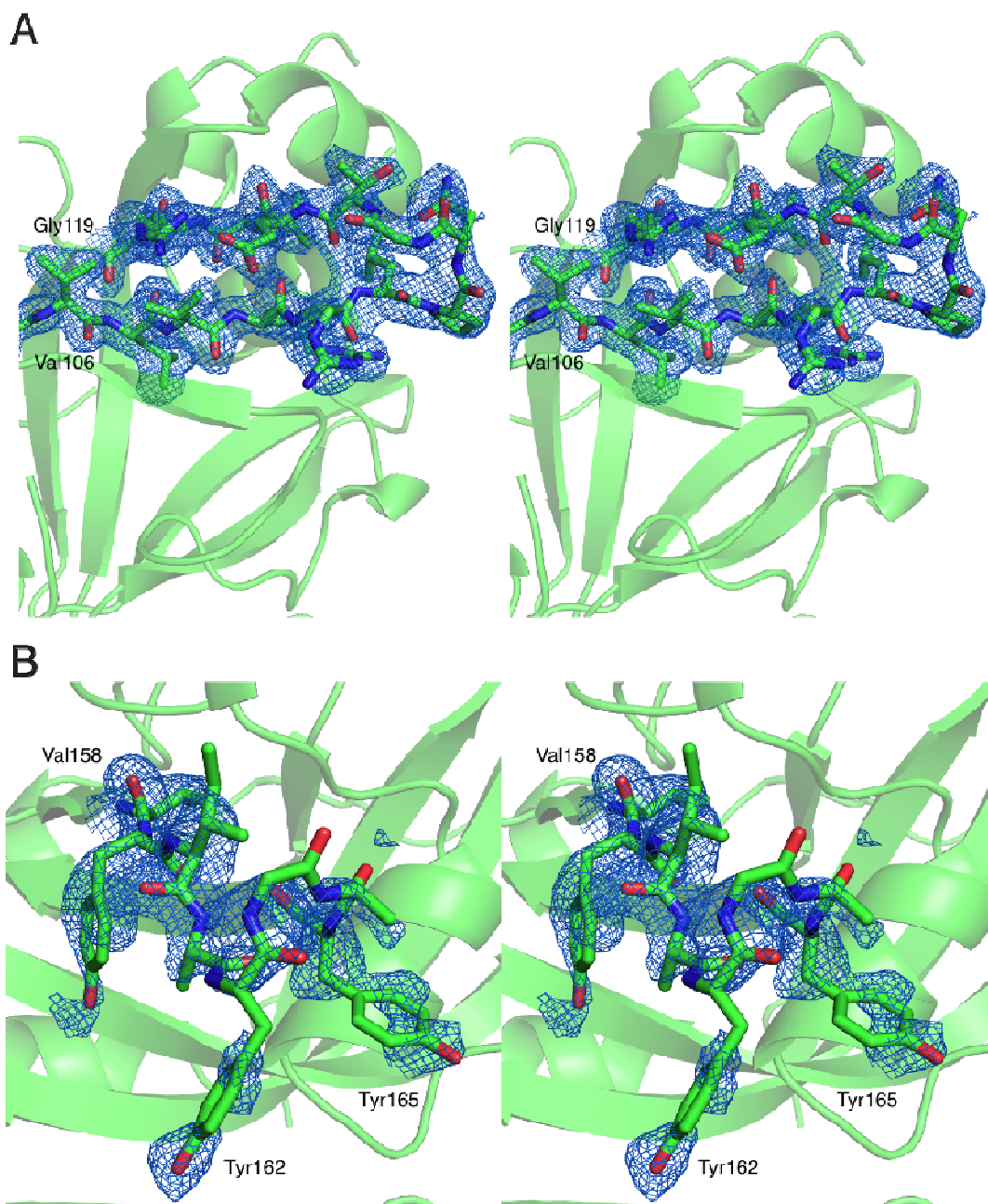


**Figure S4.** Wall-eye stereoviews of electron density in the lower-affinity  $\Delta 79\text{AAG}$  structure. (A)  $2F_o - F_c$  electron density omit map (blue mesh) contoured at  $1\sigma$  around Val106-Gly119 shows representative electron density. (B)  $2F_o - F_c$  electron density omit map (blue mesh) contoured at  $1\sigma$  shows the region from Val158-Tyr165. This Tyr162 loop is flexible, displaying broken electron density and higher B-factors (2-fold higher than the chain average; this same loop in the high-affinity pseudo-duplex  $\epsilon\text{C}$  structure shows average B-factors). The absence of these residues results in the appearance of positive difference electron density, while refinement in the presence of the modeled residues does not yield negative difference electron density. Thus, these residues are included in the model as depicted. Non-carbon atoms are colored as in Figure S1.

## References

1. Lau, A. Y., Wyatt, M. D., Glassner, B. J., Samson, L. D., and Ellenberger, T. (2000) Molecular basis for discriminating between normal and damaged bases by the human alkyladenine glycosylase, AAG, *Proc. Natl. Acad. Sci. USA* 97, 13573-13578.
2. Lingaraju, G. M., Davis, C. A., Setser, J. W., Samson, L. D., and Drennan, C. L. (2011) Structural basis for the inhibition of human alkyladenine DNA glycosylase (AAG) by 3,N4-ethenocytosine containing DNA, *J. Biol. Chem* 286, 13205-13213.